SPACE-TIME VARIATIONS IN WATER VAPOR AS OBSERVED BY THE UARS MICROWAVE LIMB SOUNDER

Lee S. Elson, William G. Read, Joe W. Waters

Jet Propulsion Laboratory, California Institute of Technology, Pasadena, CA

Philip W. Mote, Jonathan S. Kinnersley and Robert S. Harwood

Edinburgh University, Edinburgh, UK

May 1, 1995

ABSTRACT

Water vapor in the upper troposphere has a significant impact on the climate system. Difficulties in making accurate global measurements have led to uncertainty in understanding the coupling to the hydrologic cycle in the lower troposphere and to water vapor's role in radiative energy balance. The Microwave Limb Sounder (MLS) on the Upper Atmosphere Research Satellite (UARS) is able to provide information on water vapor concentration in the upper troposphere. These measurements have good sensitivity and nearly global coverage. An analysis of preliminary Retrievals based on three years of observations shows the water vapor distribution to be similar to that measured by other techniques and to model calculations. The emphasis here is on the time variation of the zonal mean as well as spectral characteristics of zonally-asymmetric propagating disturbances.

The primary measurements of water vapor made by the MLS instrument were in the stratosphere where this species acts as a conserved tracer under certain conditions. This characteristic allows a qualitative diagnosis of preferred directions for transport by waves as well as an understanding of transport by longer period oscillations such as the semi-annual oscillation (SAO) in the upper stratosphere and the quasi-biennial oscillation (QBO) in the lower stratosphere. Part of the discussion here focuses on the time variability of the zonal mean and zonally-varying stratospheric water vapor over an approximate 19 month period beginning, in October of 1991. The. SAO is shown to be variable with a large amplitude during the early part of the UARS mission. Comparisons with model calculations show general agreement with some differences in the amplitude and phase of long- term variations. Equatorial water vapor variations in the lower stratosphere suggest the presence of meridional transport.

1. Introduction

Water vapor (H_2O) plays several important roles in the atmosphere. In the troposphere, phase changes and radiative properties cause it to dominate processes crucial to energy balance. Therefore, knowledge of its current and future distribution is central to the determination and prediction of climate change. This is especially true of the upper troposphere where there is some controversy over *Lindzen's [1990]* argument that increased surface temperatures are likely to result in a decrease in H_2O. *Gutzler* [1993] reported that current uncertainty in upper tropospheric humidity (UTH) results in an uncertainty in the upward-directed infrared radiance at the tropopause which is of the same magnitude as the radiative change due to a doubling of carbon dioxide. Clearly, the extent to which upper tropospheric water vapor is coupled to boundary layer convection is important in studies of climate and climate change.

The upper troposphere acts as a crucial link between the surface, where many wave variations have their origins, and the stratosphere where changes are driven mostly by wave activity. Good examples of this are the semi-annual and quasi-biennial oscillations (SAO and QBO) which are influenced by upward propagating planetary waves. The detection and quantification of such waves help to complete our understanding of how changes are forced in the stratosphere. The upper troposphere also exhibits shorter period oscillations such as the 30- 60 day or Madden and Julian oscillation[*Madden and Julian, 1994]* which are driven by and indicative of interactions between convection and the circulation.

Water vapor, like related quantities such as rainfall, varies on a variety of spatial and temporal scales. This can make observations difficult to interpret. In the upper troposphere, *in situ* measurements provide high vertical resolution but horizontal coverage is limited due in part to operational shortcomings of relative humidity sensors on conventional radiosondes [*Wade*, 1994]. From other measurements such as lidar and Loran

tracked soundings [*Soden, et al.,* 1994], we know that UT'H can have vertical structure of order one kilometer, especially in the vicinity of ice clouds which act as a vapor source [*Smith et al., 1994].* Such variability cannot be well characterized by satellites, which offer a growing set of UTH observations. Satellites offer much greater potential for significant horizontal and temporal coverage and resolution. Their observations can be separated into two categories: nadir and limb measurements. Nadir viewing instruments can be further sub-divided according to whether they are in low or high orbit. High orbit, geostationary sensors such as the GOES 6.7 μm channel make possible the determination of UTH[*Soden and Bretherton, 1993, Udelhofen and Hartmann,*1995] and offer excellent (-1 0 km) horizontal resolution but limited horizontal coverage. GOES is sensitive to UTH between 500 and 200 hPa (5.5-12 km) and therefore may not be able to distinguish between vertical variations cm smaller scales and horizontal or temporal variations. Similar restrictions apply to H_2O retrieved from the High Resolution Infrared Radiation Sounder 2 (H IRS2) on the low altitude, polar orbiting TI ROS satellites [*Susskind,*1993]. HIRS2 observations, because of the orbit, cover the entire globe daily but the effective horizontal resolution is less than that of GOES. Although the field of view (FOV) is of order 10-50 km, retrievals have a spacing of about 250 km{*Susskind et al., 1984].*

Limb sounders provide better vertical resolution than nadir sounders. The Microwave Limb Sounder (MLS)[*Barath et al., 1993]* on the Upper Atmosphere Research Satellite (IJARS) was designed to sense water vapor in the stratosphere using measurements at 1 83 GHz [*Lahoz et al.*, 1995b]. Its 205 GHz radiometer has sensitivity to H_2O in the upper troposphere where the. concentration is in the range 100-300 ppmv [*Read et al.*, 1995]. In the polar regions, where the tropopause is low, these measurements are in the stratosphere. Preliminary values of water vapor retrieved using this radiometer are presented here. While the failure of the 183 GHz radiometer in April, 1993 limits the stratospheric H_2O data set to about 19 months, the 205 GHz radiometer has made three years of nearly continuous measurements and continues to function. With a 3 km FOV in the vertical and

retrievals which have little degradation due to cirrus clouds, MLS provides a water vapor data set with some advantages over those previously mentioned. There are also some disadvantages. Like most limb sounders, horizontal resolution in the cross-track direction is limited by the orbital spacing and therefore by the orbital period. For MLS, there are about 15 orbits per clay with adjacent orbits separated by about 2670 km at the equator. Although the preliminary H_2O retrievals discussed here have not yet been systematically validated, *Read et al.* indicate that the comparison between daily MLS H_2O observations and model, satellite and *in situ* values is quite good. *Read et al.* also compared horizontally binned data for 3 month periods with cloud climatologies and found that the two had similar morphologies. *Elson et al. [1994b]* compared "synoptic" (see section 2) maps of MLS water vapor with the GOES data described above and found the morphological agreement to be reasonable given the significant differences in horizontal and temporal resolution in the two data sets.

In the stratosphere, the circulation is frequently described in terms of a residual mean circulation which, at low altitudes, consists of upwelling at low latitudes and a downward return flow at high latitudes. Superimposed on this flow are various cycles: the QBO, SAO and annual cycle. There have been numerous attempts to use long-lived species as tracers of motions associated with these cycles. Two factors can complicate this process. Different tracers often yield conflicting results and the cycles can influence one another. A good example of this is the QBO. The circulation associated with this phenomenon is confined to the equator and sub-tropics and is strongest between about 10 and 40 hPa [*Andrews et al., 1987],* Several workers (e.g. *Chipperfield and Gray, 1992)* have noted that the sign of the QBO anomaly for a particular tracer depends on the direction and sign of the mixing ratio gradient of that tracer. A recent publication [*Hasebe, 1994]* finds that ozone and aerosols do not give a consistent picture, of the QBO when compared with model predictions.

H_2O in the stratosphere has also been used as a tracer of air motion, since at lower

levels it is usually conserved on time scales less than about a hundred days [*Le Texier et al., 1988]*. Limb Infrared Monitor of the Stratosphere (L1 MS) observations show that the general characteristics of the vertical distribution of H_2O in the upper stratosphere are consistent with methane acting as a source [*Jones et al.,* 1986]. *Lahoz et u].,* [1995b] have shown that the 183 GHz radiometer on MLS provided H_2O measurements in the stratosphere which have, for the Version 3 data used here, a single profile precision of 5% or better and an accuracy of 1.2 ppmv or better between 46 hPa and .46 hPa. By comparing Version 3 retrievals with correlative data, they were able to estimate that MLS H_2O observations may be too high by about 5-2070, depending on pressure. level. This must be kept in mind when comparing MLS observations to LIMS, as is done here. Transport in the winter polar vortices was examined by *Lahoz et al., [1994,* 1995a] using individual vertical profiles of MLS H_2O along an orbit track for selected days. *Harwood et al.* [1993] studied transport of H_2O out of the vortex to mid-latitudes. Focusing. on the equatorial regions and sub- tropics, *Carr et al., [1995]* noted that MLS observations confirm a H_2O distribution generally consistent with the Brewer-Dobson circulation modulated by the annual cycle, the SAO and the QBO. They examined the lower stratosphere (pressures greater than 20 hPa), finding significant annual variations. *Mote et* al., [1995] demonstrated that these variations were largely due to the annual variation in tropical tropopause temperatures which control the mixing ratio of air entering the stratosphere.

The discussion that follows is concerned with the spatial variations of MLS H_2O in the upper troposphere and stratosphere and how these variations change with time. Past work has focused mainly on the zonal mean. We examine both the zonal mean and the deviations from the mean. Measurements in the upper troposphere are relatively new and unique. Their general characteristics will be compared with similar observations and with models. Ml .S stratospheric observations will also be compared with model calculations with emphasis on vertical displacement of 1-$1_2$0 isosu faces. Although the results presented here are meant to serve as an overview, several periods will be examined in greater

detail.

Section 2 briefly describes the analysis used with the MLS data and section 3 contains results from 3 years of upper tropospheric measurements of H_2O, including model comparisons. Section 4 examines the stratosphere at several levels in the vertical, and compares equatorial behavior with that of a 2-D model and section 5 contains a discussion of other observations and some conclusions.

2. Data analysis

The orbit of UARS causes measurements made by MLS to progress through all local solar times in about 36 days. In order for side- looking instruments to cover the high latitudes of both hemispheres, UARS performs a 180° yaw maneuver after covering all local times. The period between yaws is referred to as a UARS "month". MLS views all longitudes daily although the latitudinal sampling depends on the UARS yaw state.

One way to quantify the large scale variability of a satellite data set is to use Fourier analysis. This approach has been applied here in the time and longitude domain while spatial binning is applied to the height and latitude domains. *Elson and Froidevaux* [1993] described the technique and *Elson et* al. [1994a] applied it to ozone (O_3) variations. Specifically, this approach starts with a coordinate system rotation which allows the determination of Fourier transform coefficients of H_2O concentration for discrete values of m, the longitudinal wavenumber, and σ, the frequency at specific latitudes and heights. The use of fast Fourier transforms (FFT's) requires that data points be equally spaced in longitude and time. Because of this and variations in the UARS orbital period, analysis of data over extended periods of time is generally not possible. This variability is small enough to allow the calculation of Fourier coefficients over a 7.2 day (108 orbit) period and unless otherwise indicated, these coefficients are used here. Longer calculations (e.g. over a UARS month) are possible only during times when the orbital period is very

slowly changing.

The Fourier transform coefficients can be used to create "synoptic" maps, i.e. a gridded array calculated by inverting the coefficients for all longitudes at one time.. The 15 UARS orbits per day result in a Nyquist period near 1 day at the. equator for the smaller longitudinal wavenumbers (largest spatial scales) while the largest resolvable wavenumber (6, corresponding to about 6600 km at the equator) has a slightly longer Nyquist period. Therefore, the diurnal frequency, which could be important in the upper troposphere but not (for H_20) in the stratosphere, will not be fully resolved, resulting in the possibility of aliasing. Small spatial scale variability may cause a similar result. Despite these limitations, daily maps of water vapor in the upper troposphere (and stratosphere) appear reasonable [*Elson et al.*, 1994b]. The likely reason for this is that there does not appear to be much power at the diurnal frequency, *Udelhofen and Hartmann [1995]* found that diurnal amplitudes in UTH are typically only a few percent.

The results presented here consist largely of time variations in the zonally-averaged and zonally-varying (wavenumbers 1 -6) H_20 concentration. These variations are calculated by combining all resolved frequency contributions to the inverse transform for individual zonal harmonics. As discussed by *Elson et al.* [1994a], the Fourier transform coefficients are also used to calculate the cross-spectral and power spectral density functions, estimates of statistical significance in the form of *a posterior* probability and eastward and westward propagating wave variances described by Schäfer 11979].

3. Upper Tropospheric Results

3a. Time evolution of zonally-averaged H_2O .

The zonally-averaged (m=0) fluctuations of MLS H_2O at 215 hPa for the first 3 years of measurements are shown in Fig. 1. Missing days (e.g. UARS yaw maneuvers, MLS

field-of-view interference from the moon, platform and instrument problems) have been omitted, resulting in gaps in this and similar figures. A great deal of day to day variability, as well as a clear annual cycle are evident. The maximum in concentration occurs, as expected, in the equatorial regions and its latitude tends to follow the sun with a lag of about two months. The poleward deflection of the maximum is similar in the two hemispheres and reaches its extreme in February and August in the South and North respectively. Maximum values are usually greatest in June, July and August, as expected from the greater convective activity that occurs over land and the larger land mass in the Northern Hemisphere. A weak splitting of the maximum tends to appear in November, especially in 1991 and 1992. This is likely due to differences between eastern and western hemispheres as described in section 5a. The largest meridional gradients occur in the subtropics and there is considerable interannual variation with 1992.-1993 being wetter than 1993-1994. By "interannual variation", we mean changes occurring on time scales longer than a year which are not obviously associated with known phenomena.

Fig. 1 also shows calculations of zonally-averaged H_2O from the National Center for Atmospheric Research Community Climate Model (CCM2) which has been described by *Mote* [1995]. The overall structure of the model variations is similar to the observations however the model tends to predict a larger increase in the maximum concentration in July and August than is observed. This feature was noted by *Soden and Bretherton* [1994] in their comparison of CCM2 simulations and GOES data. *Soden and Bretherton* also suggested that the CCM2 underestimates the gradient in H_20 between the equator and subtropics due to difficulties in simulating ascent and descent in the Hadley circulation. Larger gradients and maxima closer to the equator in MLS data in July and August support this conclusion. The model also predicts a maximum in the concentration which is further north than that observed during the northern summer months. *Salathé and Chesters* [1995] and *Salathé et al. [* 1995] found similar differences when comparing TIROS Operational Vertical Sounder data with both European Centre for Medium-Range

Forecasts analyses and Goddard Laboratory for Atmospheres General Circulation Model simulations. In both cases, they found that, as here, observations tend to show more moisture where values are large. They suggest that this is due, in part, to the convective parameterization schemes used for analysis.

3b. Time evolution of zonally-varying H_2O

Significant departures from zonal symmetry in the H_2O field are also present. In searching for waves, two competing factors influence the way data are analyzed. If one is searching for short (< 10 days) period waves, it is useful to examine multiple short (<30 days) periods. The reason for this is that transience in longer records may obscure signals [*Salby et al.,* 1984]. The limited spectral resolution is not usually a serious constraint. If longer period variations, such as the 30-60 day oscillation, are to be analyzed, good spectral resolution is important and available only through the use of much longer records [*Salby and Hendon, 1994].* Because the initial stages of analysis of MLS data limit records to about 30 days, only a few attributes of long period oscillations are evident in the results below. Most of the discussion will focus on shorter period waves.

Fig. 2 shows the results of a calculation of Fourier coefficients over a UARS month (Jan. 10 to Feb. 8, 1993) at215 hPa. This time period was chosen because the slow variation of the UARS orbit makes possible an extended FFT calculation. Both eastward and westward propagating wave variances are depicted as a function of latitude and frequency for each resolvable zonal wavenumber (1 -6). Because the variance field has been spectral 1 y smoothed [*Elson et al.,* 1994a] and *the* amplitude variation with small frequency is rapid, values within one spectral bandwidth on either side of zero frequency are distorted and have been omitted. Fig. 2a (wave 1) indicates the presence of the diurnal signal which, as discussed above, may be aliased to some extent and large amplitude variances within a few degrees of the extremes in latitude coverage are possibly artifacts of the

transform process [*Elson and Froidevaux, 1993]*. This figure reveals that for small wavenumbers (large scales) most of the power is present at low frequencies and that most of these long period disturbances propagate eastward. The latitudinal extent of all disturbances is quite limited. The larger wavenumbers show evidence of faster, primarily eastward moving peaks with periods as short as about 1,5 days. Calculations of *a posteriori* probability, made from estimates of coherency, show that nearly all peaks are statistically significant at the 90% or greater level. One other month (Aug. 13- Sept. 20, 1992) has been examined and shows similar behavior for low frequencies but fewer high frequency variations.

4. **Stratospheric Results**

4a. Time evolution of zonally-averaged H_2O .

The zonally-averaged (m=0) fluctuations of H_2O during 1991 and 1992 are shown in Fig. 3 for four different levels in the stratosphere. Several features are prominent in the data. In the equatorial region, the SAO becomes more visible as one progresses upward in the atmosphere. At 2 hPa the SAO dominates the pattern between 30° N and 30° S but is replaced by an irregular annual variation in the polar region. This annual component is due, in part, to downward motion there [*Lahoz et al.,* 1994]. As high H_2O values descend, concentrations at 2 hPa increase. At low latitudes, there is also evidence of interannual change at all levels. This is obvious at 46 hPa where there appears to be a trend towards lower water vapor values. The opposite appears true at 1() and 2 hPa. As noted by *Carr et al., [* 1995] the mixing ratio at 22 hPa shows no overall trend, but does have a variation that is not annual. Extreme dehydration is evident at 46 hPa in August and September of 1992. This is expected because of removal of H_2O by '1 ype II polar stratospheric clouds [e.g. *Drdla and Turco, 199 1].*

Another view of the SAO is provided by a time series plot versus altitude at the equator-. Figs. 4c and 4d show the zonally-averaged MLS H_20 observations, and, in Fig. 4e the results from a two- dimensional (2-D) model simulation for one year starting on UARS clay 1 (Sept. 12, 1991). The model is an improved version of that described by *Kinnersley and Harwood [1993]* which has a prescribed water vapor mixing ratio at the 60 km (-.2 hPa) level and at the tropopause. The general form of the observations and model agree, The most obvious differences are in the amplitude of variations, or the displacement of the isopleths in the upper stratosphere, and in the timing of the second maximum (June or July in the observations, April or May in the model). The observed amplitudes are larger than the model above about 4 hPa. At 10 hPa the model shows variations on a time scale of a few months that do not appear in the first 10 months of observations.

4b. Time evolution of zonally-varying H_2O.

Fig. 5 shows the absolute value of wavenumber 1 variations, at pressure levels of 46, 10 and 2 hPa. Wave activity is strongest at high latitudes in the fall, winter and spring months, but occurs in bursts lasting from one to several weeks. Of the three levels, 10 hPa exhibits the largest amplitude. Fig. 5 may be direct] y con pared with 1 ig. 1 of *Elson et al.* [1994a] which shows m= 1 variations in 0_3. The overall structure of variations is similar for the two species, however an examination of specific events shows that the relative amp] i tude is often larger in one species than the other. Which spc.tics has the stronger response depends on factors which influence the concentration. At 2 hPa, 0_3 is primarily photochemically controlled and H_20 is primarily dynamically controlled so that a large temperature amplitude in the absence of large winds might be expected to produce larger O_3 variations. At lower altitudes, where both species are dynamical y controlled, differences are due to the background (zonally-averaged) distribution of the two species in the presence of transport. For example, at 46 hPa, the wate vapor wave 1 amplitude is large

near 60° in May, 1992 (marked with a red arrow in Fig. 5e). The O_3 amplitude for the same time and place is small. An examination of a vertical cross section of the zonal mean of the two species, in Fig. 6, shows why this occurs. The distribution of O_3 is not unusual, with relatively small meridional gradients in this region. The H_2O distribution, however, shows a small anomalous peak near 60° with isopleths nearly perpendicular to those of O_3 . The associated increase in meridional gradient equatorward of this feature means that a zonally - asymmetric meridional wind is more likely to produce meridional transport, and a zonal asymmetry in the distribution. An examination of National Meteorological Center data shows an enhancement in the meridional wind at this time and place.

At higher altitudes, water vapor is conserved over a period of several weeks, and can therefore act as a tracer of atmospheric motions for these time scales. For example, in Fig. 5 at 2 hPa, the wave 1 amplitudes for days 338-375 show considerable activity near 60°S. During this UARS month, the orbital period was stable enough to allow the calculation of one set of Fourier coefficients for the entire month. Fig. 7 shows both the zonal mean and wave 1 variance for a part of the spectrum centered on an eastward 10 day period . The region near 2 hPa, which shows a peak in the variance, corresponds to the region which has the largest component of zonal mean gradient in the meridional direction. Therefore, it is likely that meridional transport is effective at this time and place. The results for m=2 fluctuations (not shown) are similar in structure to those for m= 1 but the amplitudes are generally smaller.

5. Discussion

5a. The Upper Troposphere

The tropospheric variations in zonal mean H_2O shown above are similar to the HIRS2 results of *Susskind [* 1993, Fig. 7b], given the differences in measurement technique and geometry. The implication from the 3 years of MLS data and 1 year of HIRS2 data is that the seasonal variations and hemispheric asymmetries depicted are fairly robust features. *Susskind* also used HIRS2 data to show that hemispheric asymmetries in the seasonal variation of zonal mean H_20 are dependent on the longitude range over which the average was calculated. For example, he found that most of the difference in peak values between January and July are due to differences in the longitude range from 150° west eastward to 30° east. *Soden and Bretherton [1994]* noted substantial differences between mid- latitude GOES UTH data over this region and SAGE II (Stratosphere Aerosol and Gas Experiment) observations which covered all longitudes. Satellite observations of the location of the intertropical convergence zone [*Waliser and Gautier*, 1 993] also show hemispheric asymmetries. A global average of 17 years of highly reflective cloud data bear a striking resemblance to Fig 1.

Departures from zonal symmetry have been detected in several data sets sensitive to the upper troposphere. Studies have used outgoing longwave radiation (OLR) [e.g. *Salby and Hendon, 1994]* as an indicator of cloudy convection and generally show eastward propagating variances with a wide range of periods and largest amplitudes in wavenumbers 1-3. As discussed above, the analysis here does not have the spectral resolution to characterize the prominent spectra] peaks in the 30-60 day range which are evident in the OLR data, however the meridional structure of the low wavenumber eastward variance in Figs 2a-2c is quite similar that seen in low frequency OLR results. The isolated eastward peaks near 8 days and about 40°S latitude in Figs. 2a, 2b and 2d are similar to a peak found by *Salby et* u/. [1991] in Pacific area OLR data, and is probably indicative of a disturbance with significant amplitude in the western pacific region discussed above. A period of 8 days is close to that of a spectral peak found by *Zangvil and Yanai [* 1980] in upper troposphere wind data. They attribute this peak to Kelvin waves, partly because of

the symmetry of the disturbance about the equator. Such an assignment is not appropriate for the results discussed here.

There have been numerous studies of upper tropospheric variations using wind data. The general characteristics of wind spectra differ from the water vapor results mainly in the sub-tropics where the former have larger amplitudes. Zonal wind spectra generally show significant amplitude at long (> 15 day) periods with occasional signatures of shorter period eastward propagating Kelvin waves as mentioned above. Meridional winds show little long period variation but do show peaks at shorter periods and wavelengths *(e.g. Yanai and Lu,* 1983). Unlike the results shown here and OLR data, shorter period meridional wind variations tend to favor westward propagation. In some cases, the westward propagating disturbances have been identified as mixed Rossby-gravity waves which have smaller vertical structure (4-8 km) than do eastward propagating Kelvin waves. It may be that the former are not as easily resolved in MLS data. On the other hand, OLR and water vapor are related to convection which, although affected by the circulation, is mainly influenced by the hydrologic cycle. Thus winds and water vapor may be sensitive to different types of disturbances, *Salby and Hendon, [1994]* found this to be true of the long period oscillations in OLR and wind data.

5b. The Stratosphere

The 19 months of stratospheric H_2O data allow excellent characterization of variations on time scales of a year or less. Quantitative estimates of long period variations such as the QBO, require many years of data for an accurate assessment of their effects. However, by examining H_2O together with O_3 and theoretical estimates of the circulation, it is possible to draw some conclusions about the QBO and other long period changes.

Froidevaux et al. [1994] suggested that there is evidence of the QBO in MLS

observations of 46 hPa O_3. Part of this evidence rests with a splitting of the equatorial field, in the summer and fall of 1992, so that subtropics] values are lower than those on the equator. This is consistent with a secondary circulation cell which exhibits downward motion at the equator and upward motion in the subtropics. There is also evidence of this, albeit much weaker, in the 46 hPa H_20 field (Fig. 3h) in October, 1992. *Froidevaux et al.* pointed out that the entire O_3 record is consistent with the modulation of equatorial upwelling with a QBO-like periodicity. However, the trend in H_2O at 46 hPa (Figs. 3g and 3h) is opposite to that of O_3. To investigate this, it is useful to examine the vertical variation of the two species.

Figs 4a-4c compare zonally-averaged H_20 and 0_3 at the equator versus time. The vertical displacement of H_20 isopleths is much greater than that of O_3, especially after September 1992. This cannot be explained solely by vertical motions, or, at lower levels by chemical sources or sinks. The displacement of isopleths depends in part on the relative angle between the wind velocity vector and the gradient in mixing ratio. Since the H_2O gradient has much more of a meridional component than O_3, (see Fig. 6) it is more sensitive to meridional motions than is O_3. A quantitative understanding of the role of meridional transport requires the use of a suitable transport model,

Higher in the stratosphere, interannual effects modulate the SAO. Some measure of this can be obtained by comparing MLS results with the LIMS observations of 1978/79. The zonal mean concentration at the equator, shown in Fig. 4, is similar to that of L] MS, shown in Fig. 9- 24 of the WMO report [1986]. LIMS results, like the model results in Fig. 4, show smaller variations at 2 hPa than does Ml S. This, coupled with evidence (Fig. 3) that the amplitude of the SAO decreased significantly after the first year of MLS observations, suggests that 199 1/1 992 may have been an anomalous year. Further evidence for this conclusion comes from the analysis of *Eluszkiewicz et al.* [1995] who found that the SAO in O_3 at 2 hPa decreased substantially during the September 1992 through March 1993 time period, although a stronger SAO appears later in the MLS O_3

record. *Ray et al.* (1994) pointed out that the relationship between SAO temperature and O_3 amplitudes is not easy to understand. At 2 hPa, where the two should be anti-correlated due to photochemistry, the phase difference is about one month instead of three, suggesting that transport may play a role in the O_3 distribution. At 10 hPa, *Ray et al.* concluded that the residual mean vertical velocity is incapable of accounting for the O_3 distribution through advection of NO_x.

A somewhat different conclusion has been reached by *Stott and Pardaens* [manuscript in preparation] who found that they could explain the observed meridional structure of zonally-averaged H_2O in the equatorial stratosphere. They used the UK Universities Global Atmospheric Modelling Programme GCM which produces time/height results similar to the 2-D model results in Fig. 4e, except that the phase of the SAO near 1 hPa agrees more closely with the MLS observations. The amplitude of the displacement of H_2O isopleths is quite similar in the two models and smaller than that of the observations. Neither model produces a phase variation with height which resembles that of the observations. This may be partly due to the course (~5 km) resolution of the MLS retrievals.

H_2O in the upper stratosphere is produced through the oxidation of methane [*Le Texier et al.*, 1988]. This process is rapid enough to be observed on time scales greater than a few months. Since methane is a source of water, one might expect the H_2O observations to show a more rapid increase than decrease at high levels. Such does not appear to be the case. Whether the distribution of methane and the seasonal variation in its photochemical destruction can account for some of the behavior discussed above remains to be determined.

The above discussion leaves open the question of whether the large observed SAO variations in H_2O (relative to models) are caused by an enhanced residual circulation. *Stott and Pardaens* suggested that upper stratospheric interannual variations seen in the UGAMP GCM are caused by variations in gravity and Kelvin wave forcing. Clearly

forcing of the SAO is an important factor in "tuning" models so that they resemble the observations. *Randel et al.*, [1994] reached a similar conclusion by comparing CCM2 simulations with UARS N_2O observations. Inclusion of other quasi-conserved species as tracers in these models will help to constrain them. Methane and nitrous oxide, both measured by UARS, are good candidates for such a procedure.

Acknowledgments. The authors thank the UARS project and the MLS team for providing support. This research was sponsored by NASA's Upper Atmosphere Research Satellite Project and was performed at the Jet Propulsion Laboratory, California institute of Technology under contract with the National Aeronautics and Space Administration.

REFERENCES

Andrews, D. G., J. R. Holton and C. B, Leovy, *Middle Atmosphere Dynamics,* Academic Press, Orlando, FL, pp3 13-342, 1987.

Barath, F. T., M. C. Chavez, R. E. Cofield, D. A. Flower, M. A. Frerking, M. B. Gram, W. M. Harris, J. R. Holden, R. F. Jarnot, W, G. Kloezeman, G. J. Klose, G. K. Lau, M. S. Loo, B. J. Maddison, R. J. Mattauch, R. P. McKinney, G. E. Peckham, H. M. Pickett, G. Siebes, F. S. Soltis, R. A. Suttie, J. A. Tarsala, J. W. Waters, and W. J. Wilson, The Upper Atmosphere Research Satellite Microwave Limb Sounder Instrument, *J. Geophys. Res.*, 98, 10,751-10,762, 1993.

Carr, E. S. R. S. Harwood, L. Froidevaux, R. F. Jarnot, W. A, Lahoz, Mote, P. W., A. O'Neill, G. E. Peckham, W. G. Read, R. Swinbank, R. A. Suttie, and J. W. Waters, Tropical stratospheric water vapor measured by the Microwave limb Sounder (MLS), *Geophys. Res. Lett.*, in press, 1995.

Chipperfield, M. P. and L. J. Gray, Two-dimensional model studies of the interannual variability of trace gases in the middle atmosphere, *J. Geophys. Res.*, 97, 5963-5980, 1992.

Drdla, K. and R. P. Turco, Denitrification through PSC formation-A 1-11 model incorporating temperature oscillations, *J. Atmos. Chem.*, 319-366, 1991.

Elson, L. and L. Froidevaux, The use of Fourier Transforms for asynoptic mapping: Applications to the Upper Atmosphere Research Satellite Microwave Limb Sounder, *J. Geophys. Res.*, **98**, 23039 -23049," 1993.

-----, G. L. Manney, L. Froidevaux, and J. W. Waters, Large-scale variations in ozone from the first two years of UARS MLS data, *J. Atmos. Sci.*, **51, 2X67-2876, 1994a.**

-----, W. G. Read and J. W. Waters, Daily, seasonal and interannual variations in upper troposphere water vapor as observed by UARS microwave limb sounder, paper presented at the *Chapman Conference on Watt)r Vapor in the Climate System,* Am.

Geophys. Union, Jekyll Island, GA. October 25-28, 1994b.

Eluszkiewicz, J, D. Crisp, R. W, Zurek, L. S. Elson, E. F. Fishbein, L. Froidevaux, J. W. Waters, R. S. Harwood, G. E. Peckham, R. G. Grainger and Alyn Lambert, Residual circulation in the stratosphere and lower n iesosphere as diagnosed from Microwave Limb Sounder data, *J. Atmos. Sci.*, submitted, 1995.

Froidevaux, L., J. W. Waters, W. G. Read, L. S. Elson, D.A. Flower, and R. F. Jarnot, Global ozone observations from UARS MLS: An overview of zonal mean results, *J. Atmos. Sci.*, 51,2846-2866, 1994.

Gutzler, D. S., Uncertainties in climatological tropical humidity profiles - some implications for estimating the greenhouse-effect, *J. Clint., 6, 978-983,* 1993.

Harwood, R. S., E. S. Carr, L. Froidevaux, R. F. Jarnot, W. A, Lahoz, C. L. Lau, G. E. Peckham, W. G. Read, P. D. Ricaud, R, A. Suttie, and J. W. Waters, Springtime stratospheric water vapour in the southern hemisphere as measured by MLS, *Geophys. Res. Lett.* , **20**, *1235-1238, 1993.*

Hasebe, F., Quasi-Biennial oscillations of ozone and diabatic circulation in the equatorial stratosphere, *J. Atmos. Sci.*, **51**, 729-745, 1994.

Kinnersley, J. S. and R. S. Harwood, An isentropic two-dimensional model with an interactive parameterization of dynamical and chemical planetary-wave, fluxes, *Q. J. Roy. Met. Soc.*, **119, 1167-** 1193, 1993.

Lahoz, W. A., A. C) 'Neil], E. S. Carr, R. S. Harwood, L. Froidevaux, W. G. Read, J. W. Waters, J. B. Kumer, J. L. Mergenthaler, A. E. Rochc, G. E. Peckham, and R. Swinbank, Three-dimensional evolution of water vapour distributions in the northern hemisphere as observed by Ml S, *J. Atmos. Sci.*, 51, 2914-2930, 1994.

-----, -----, H. MacLean, R. Swinbank, R. S. Harwood, L. Froidevaux, W. G. Read, J. W. Waters, J. B. Kumer, J. L. Mergenthaler, A. E. Roche, and G. E. Peckham, Three-dimensional evolution of water vapour distributions in the southern hemisphere as

observed by the Microwave Limb Sounder, *Q. J. Roy. Met. Sm.*, submitted, 1995a,

-----, M. R. Suttie, L. Froidevaux, R. S. Hat-wood, C. L, Lau, T, A. Lungu, G. E. Peckham, H. C. Pumphrey, W. G. Read, Z. Shippony, R. A. Suttie, and J. W. Waters, Validation of UARS MLS 183 GHz H_2O Measurements, *J. Geophys. Res.*, submitted, 1995b.

Le Texier, H., S. Solomon and R. R. Garcia, The role of molecular hydrogen and methane oxidation in the water vapour budget of the stratosphere, *Q. J. Roy. Met. Sot.*, **114**, 281-295, 1988

Lindzen, R. S., Some coolness concerning global warming, *Bull. Amer. Meteor. Sot.* , **71, 288-299, 1990.**

Madden, R. A., and P. R. Julian, Observations of the 4()-50 day tropical oscillation- a review, *Mon. Wea. Rev.*, 122, 814-837, 1994,

Mote, P. W., The annual cycle of stratospheric water vapor in a general circulation model, *J. Geophys. Res.*, in press, 1995.

-----, K. H. Rosenlof, J. R. Holton, R. S. Harwood, and J. W. Waters, Seasonal variation of water vapor in the tropical lower stratosphere, *Geophys. Res. Left., in* press, 1995.

Randel, W. J., B. A. Bovine, J. C. Gille, P. L. Bailey, S. T. Massie, J. B. Kumer, J. L. Mergenthaler and A. E. Roche, Simulation of stratospheric N_2O in the NCAR CCM2: Comparison with CLAES data and global budget analyses, *J. Atmos. Sci.*, 51, 2834-2845, 1994.

Ray, E., J. R. Holton, E. F. Fishbein, L. Froidevaux, and J. W. Waters, "l'he tropical semiannual oscillation in temperature and ozone observed by the ML S, *J. Atmos. Sci.*, **51,3045-3052,** 1994.

Read, W. G., J. W. Waters, D. A. Flower, L. Froidevaux, R. F. Jarnot, D. L. Hartmann, R. S. Harwood, and R. B. Rood, Upper tropospheric water vapor from UARS MLS, *Bull. Amer. Met. Soc.*, submitted, 1995.

Rind, D., E.-W. Chiou, W. Chu, S. Oltmans, J. Lerner, J. Larsen, M. P. McCormick and L. McMaster, Overview of the SAGE 11 water vapor observations: Method, validation and data characteristics, *J. Geophys. Res.*, 98, 4835-4856, 1993.

Salathé, E. P., and D. Chesters, Variability of moisture in the upper troposphere as inferred from TOVS satellite observations and the ECMWF model analyses in 1989, *J. Clim.*, **8**, 120-132, 1995,

----------, D. Chesters and Y. C. Sud, Evaluation of the upper- tropospheric moisture climatology in a general circulation model using TOVS radiance observations, *J. Clim.*, submitted, 1995.

Salby, M. L., D. L. Hartmann, P. L. Bailey, and J. C. Gille, Evidence for equatorial Kelvin modes in Nimbus-7 LIMS, *J. Atmos. Sci.*, **41**, 220-235, 1984.

----- and H. H. Hendon, Intraseasonal behavior of clouds, temperature and motion in the Tropics, *J. Atmos. Sci.*, **51, 2207-2224, 1994.**

----- , **H. H.** Hendon, K. Woodberry and K. Tanaka, Analysis of global cloud imagery from multiple satellites, *Bull. Amer. Meter. Sot.*, 72, 467-480, 1991.

Schäfer, J., A space-time analysis of tropospheric planetary waves in the Northern Hemisphere, *J. Atmos. Sci.*, 36, 1117-1123, 1979.

Smith, R. B., D. Rye, R. Rauber, H. Ochs and G. Kok, Measurements of deuterium and oxygen- 18 in the upper troposphere and implications for the water vapor budget of the atmosphere, paper presented at the *Chapman Conference on Water Vapor in the Climate System*, Am. Geophys. Union, Jekyll island, GA. October 25-28, 1994.

Soden, B. J. and F. P. Bretherton, Upper-tropospheric relative- humidity from the GOES 6.7 μm channel-method and climatology for July 19X7, *J. Geophys. Res.*, 98,' 16669-16688, 1993.

----- and -----, Evaluation of water vapor distribution in general circulation models using satellite observations, *J. Geophys. Res.*, 99, 187-1210, 1994,

Susskind, J., Water vapor and temperature, in *Atlas of satellite observations related to global change*, edited by R. J. Gurney, J. L. Foster and C. L. Parkinson, pp 89-128, Cambridge University Press, New York, 1993.

-----, J Rosenfield, D. Reuter and M. T. Chahine, Remote sensing of weather and climate parameters from HIRS2/MSU on TIROS-N, *J. Geophys. Res.*, **89**, 4677-4697, 1984.

Udelhofen, P. M. and D. L. Hartmann, Influence of tropical cloud systems on the relative humidity in the upper troposphere, *J. Geophys. Res.*, in press, 1995.

Wade, C. G., An evaluation of problems affecting the measurement of low relative-humidity on the United-States radiosonde, *J. Atmosp. Oc., 11, 687-7 (M, 1994.*

Waliser, D. E. and C. Gautier, A satellite-derived climatology of the ITCZ, *J. Clim.*, **6**, 2162-2174, 1993.

WMO, *A tmospheric Ozone 1985, Assessment of Our Understanding of the Processes Controlling its Present Distribution and Change,* Report No. 16, World Meteorological Organization, Washington, D. C., 1986.

Yanai, M and M-M. Lu, Equatorially trapped waves at the 200 mb level and their association with meridional convergence of wave energy flux. *J. Atmos. Sci.*, 40, 2785-2803, 1983.

Zangvil, A. and M. Yanai, Upper tropospheric waves in the Tropics. Part 1: Dynamical analysis in the wavenumber-frequency domain. *J. Atmos. Sci., 3'7,* 2X3-298, 1980.

Figure Legends

Figure 1. Time evolution of zonal mean 215 hPa h4LS water vapor (ppmv) a) for UARS days 20-375 (Oct. 1, 1991 -Sept. 20, 1992), b) for UARS days 380-736 (Sept. 25, 1992- Sept. 16, 1993), c) for UARS days 743- 1095 (Sept. 23, 1993-Sept. 10, 1994) d) for CCM2 model results.

Figure 2. Spectrally smoothed wave variance of water vapor ($ppmv^2$) at *215* hPa, *as* a function of latitude and frequency for zonal wavenumbers 1-6 [(a)-(f)]. Data from Jan. 10- Feb. 8, 1993 were used in the analysis.

Figure 3. Time evolution of zonal mean MLS water vapor (ppmv) at a) 2 hPa for UARS days 20-375, b) 2 hPa for UARS days 380-582. c) and d) are the same as a) and b) but at 10 hPa. e) and f) are the same as a) and b) but at 22 hPa. g) and h) are the same as a) and b) but at 46 hPa.

Figure 4. Equatorial zonal mean ozone (ppmv) versus pressure and time for a) the first year of MLS measurements smoothed with a 3 day running mean, b) as in a) but for the second year. c) and d) are the same as a) and b) but for water vapor. e) shows results from 2-D model calculations.

Figure 5. As in Fig. 3 but for zonal wavenumber 1 water vapor amplitude (ppmv). 22 hPa results have been omitted.

Figure 6. Zonal mean values of water vapor (a) and ozone (b) (ppmv) versus pressure and latitude for May 3-10, 1993.

Figure 7. a) Zonal mean water vapor (ppmv) versus pressure and atitude for August and September, 1992 (UARS days 33$-375, , b) as in a) but 10 d:y eastward propagating water vapor variance ($ppmv^2$).

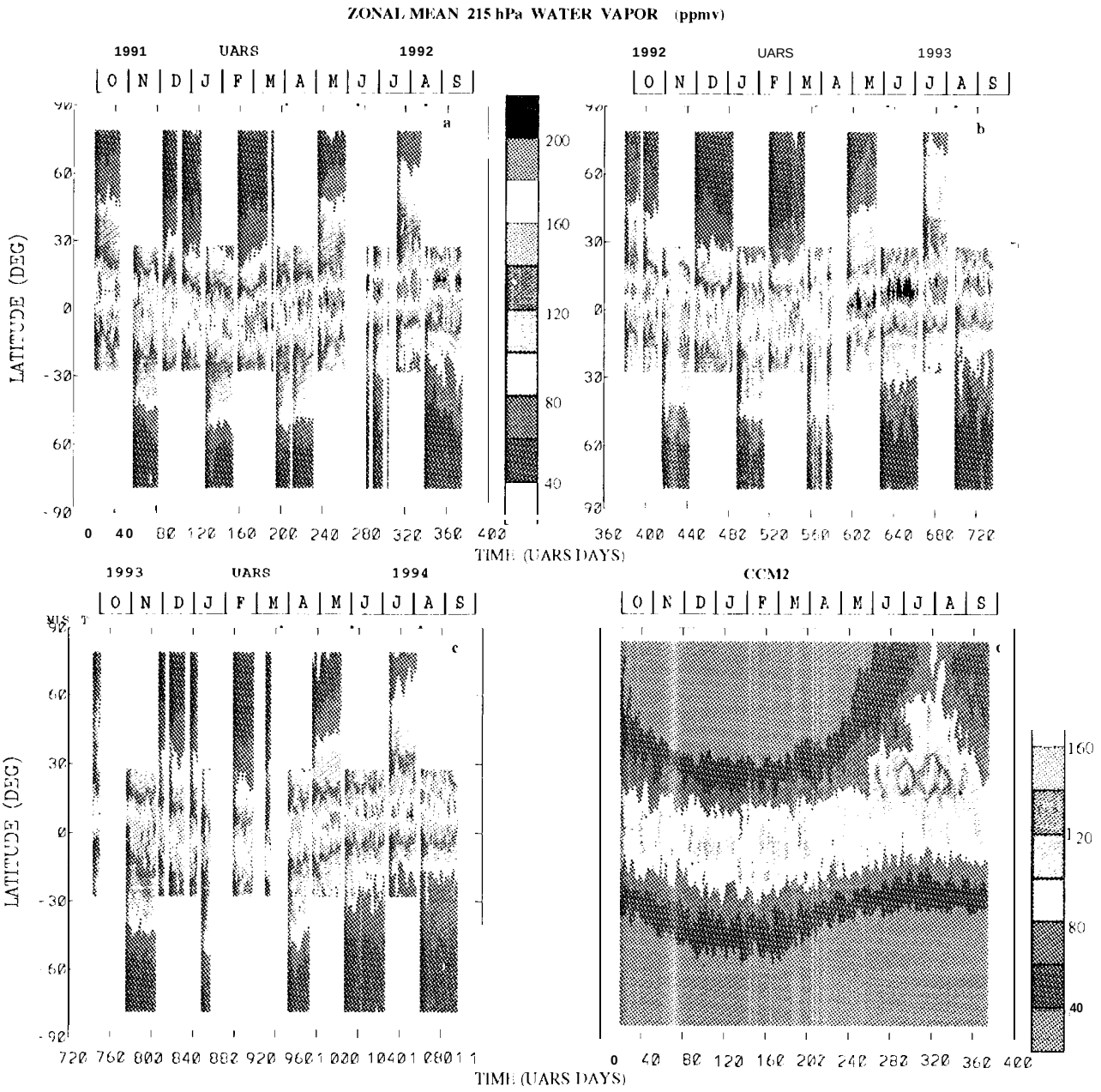
ZONAL MEAN 215 hPa WATER VAPOR (ppmv)
1991
UARS
1992
O N D J F M A M J J A S
a
1992
UARS
1993
O N D J F M A M J J A S
b
200
160
120
80
40
LATITUDE (DEG)
90
60
30
0
-30
-60
-90
0 40 80 120 160 200 240 280 320 360 400
360 400 440 480 520 560 600 640 680 720
TIME (UARS DAYS)
1993
UARS
1994
O N D J F M A M J J A S
c
CCM2
O N D J F M A M J J A S
c
160
120
80
40
LATITUDE (DEG)
720 760 800 840 880 920 960 1000 1040 1080 1120
0 40 80 120 160 200 240 280 320 360 400
TIME (UARS DAYS)

Fig1

WAVE VARIANCE OF H_2O (ppmv^2) at 21S hPa

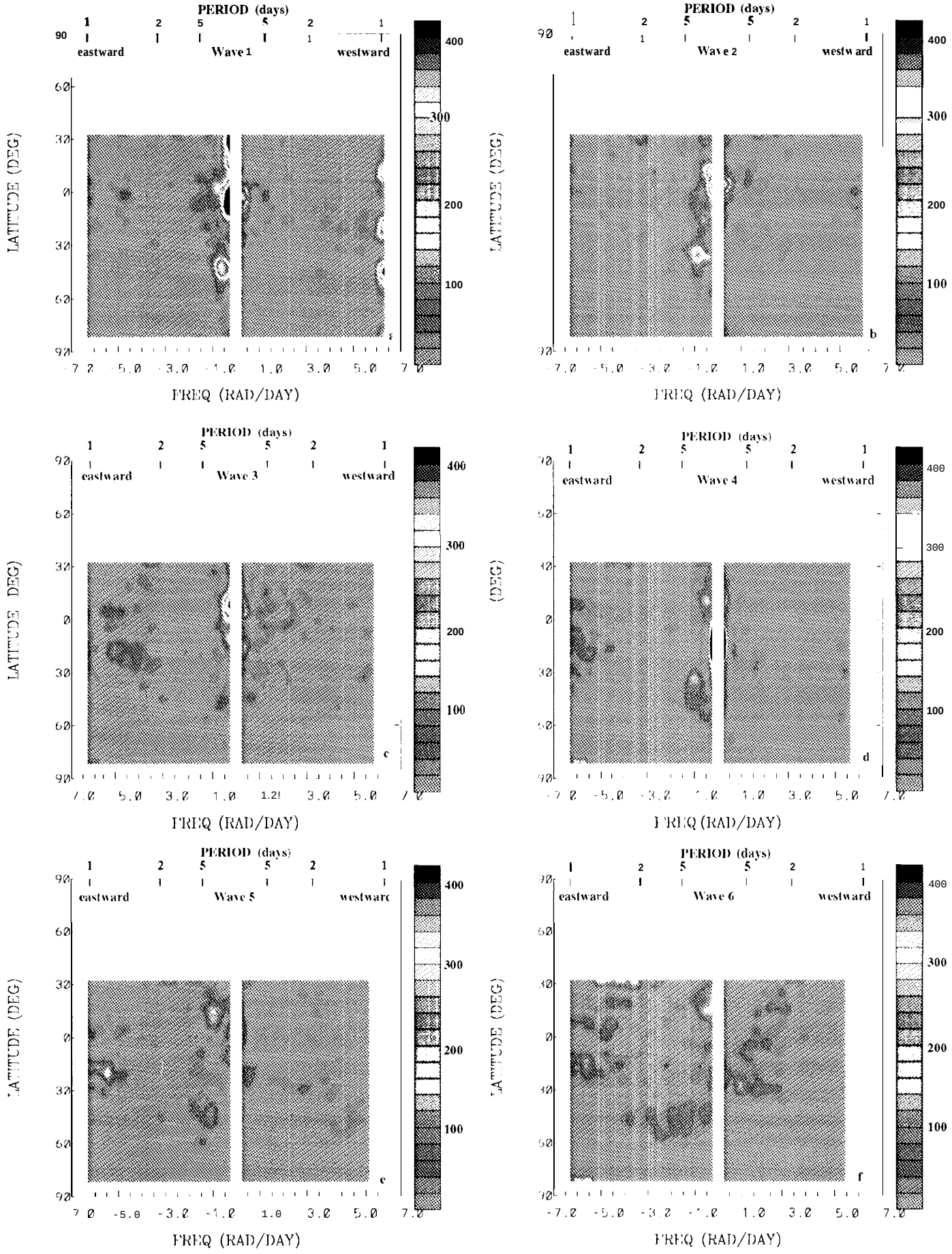

Fig 2

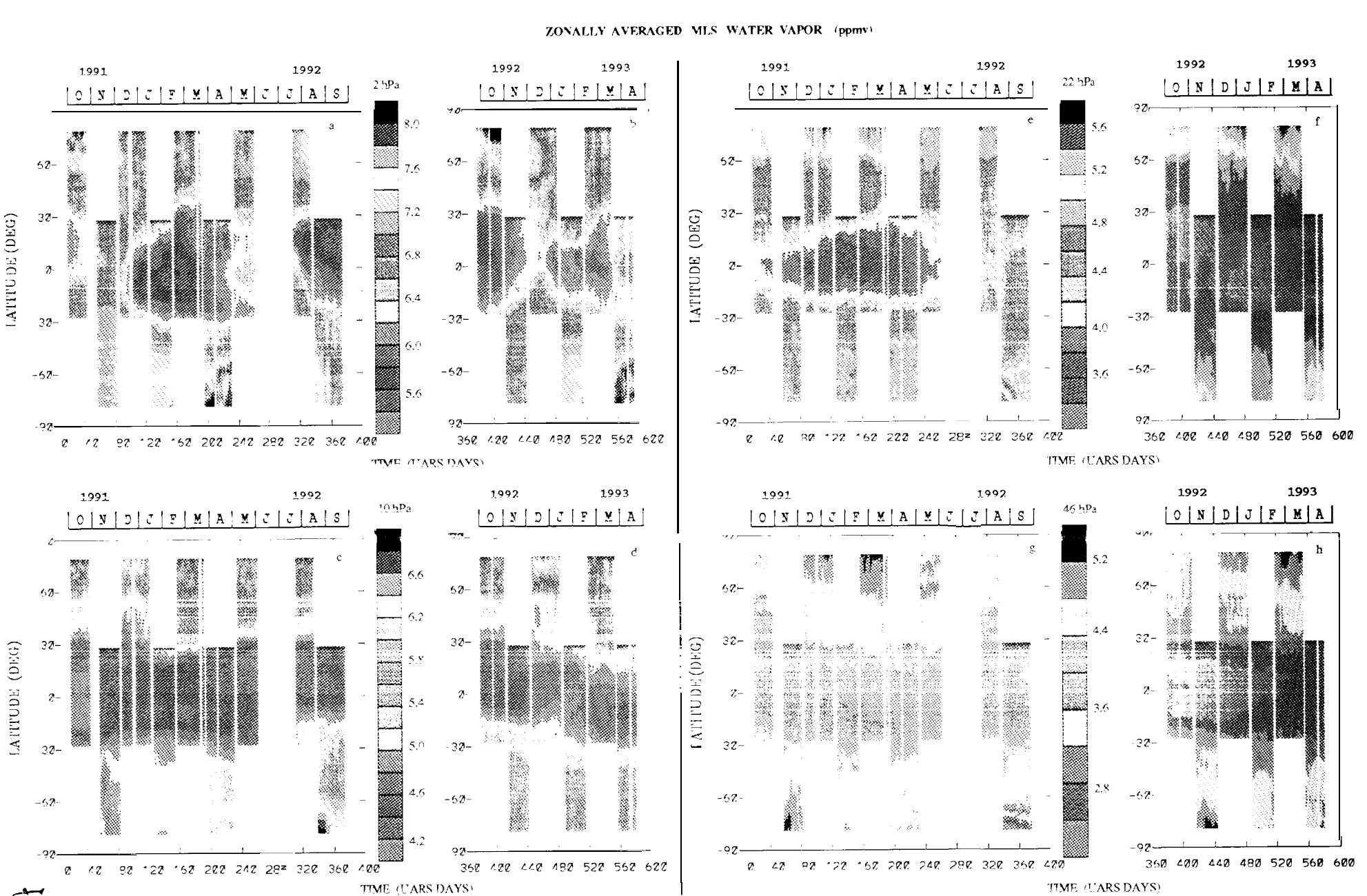
ZONALLY AVERAGED MLS WATER VAPOR (ppmv)
1991
1992
1993
O N D J F M A M J J A S
2 hPa
10 hPa
22 hPa
46 hPa
a
b
c
d
e
f
g
h
LATITUDE (DEG)
TIME (UARS DAYS)

ZONAL MEANS (ppmv)

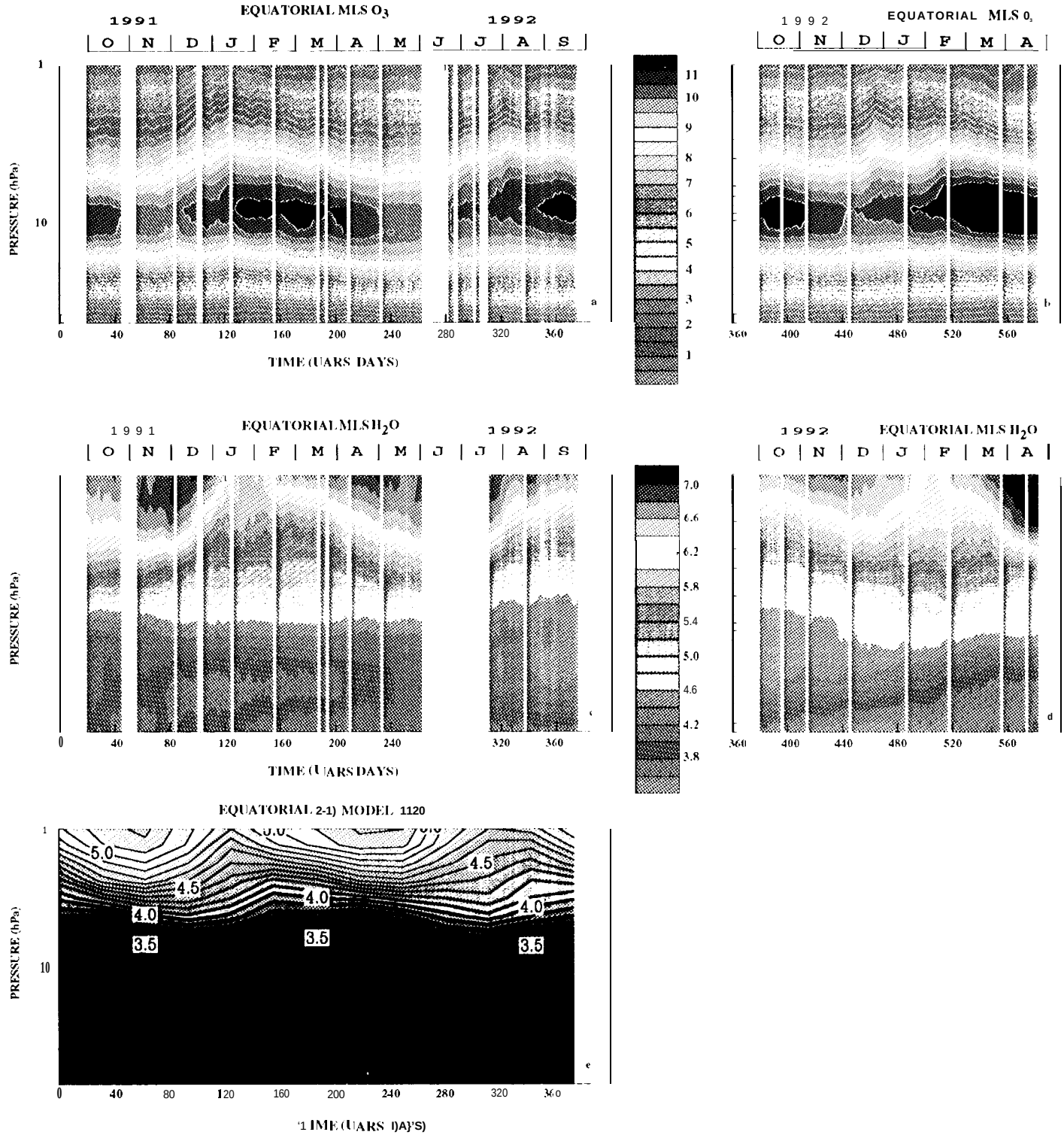

Fig 4

WAVE 1 MLS WATER VAPOR (ppmv)

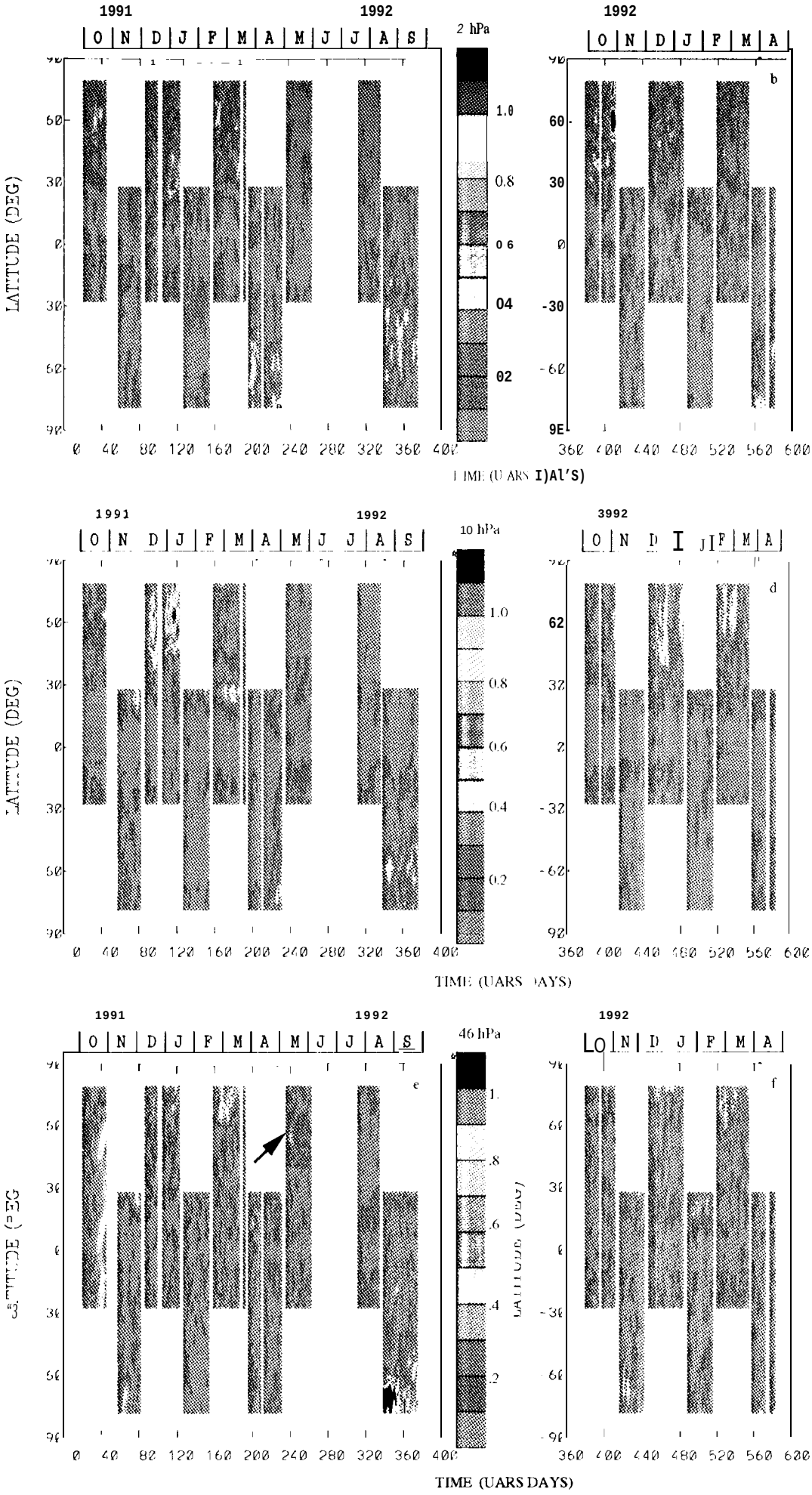

Fig 5

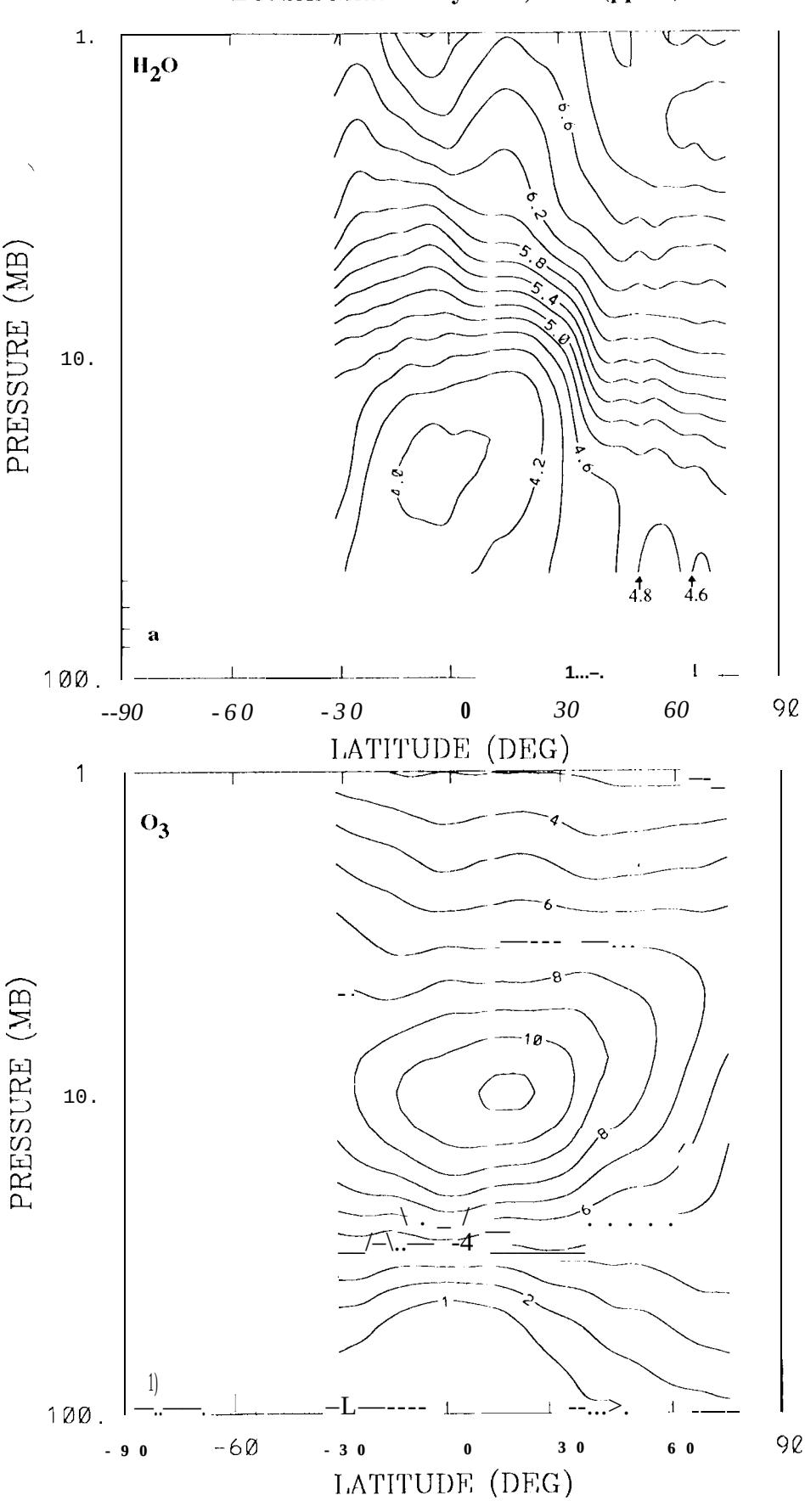
ZONAL MEAN May 3-10, 1992 (ppmv)
H_2O
PRESSURE (MB)
1.
10.
100.
6.6
6.2
5.8
5.4
5.0
4.6
4.2
4.0
4.8
4.6
a
--90
-60
-30
0
30
60
90
LATITUDE (DEG)
O_3
PRESSURE (MB)
1
10.
100.
4
6
8
10
8
6
4
2
1
-90
-60
-30
0
30
60
90
LATITUDE (DEG)

Fig 6

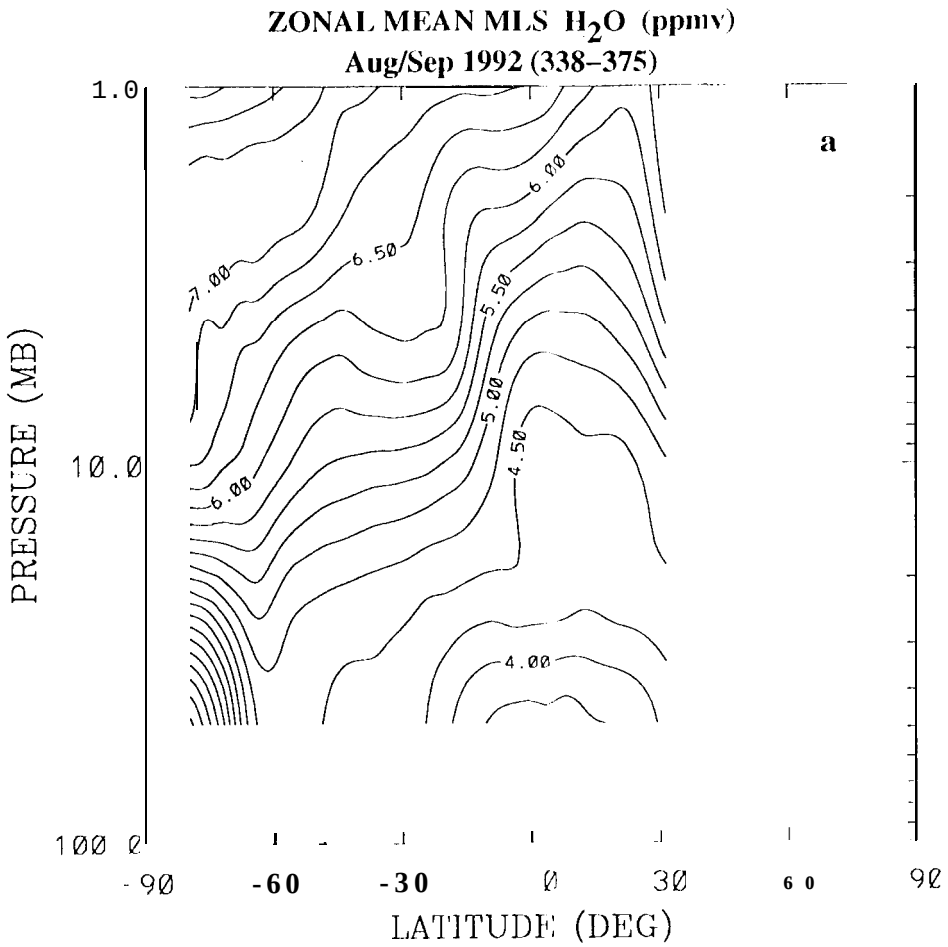
ZONAL MEAN MLS H_2O (ppmv)
Aug/Sep 1992 (338–375)
a
1.0
10.0
100 0
PRESSURE (MB)
7.00
6.50
6.00
5.50
5.00
4.50
4.00
6.00
-90
-60
-30
0
30
60
90
LATITUDE (DEG)

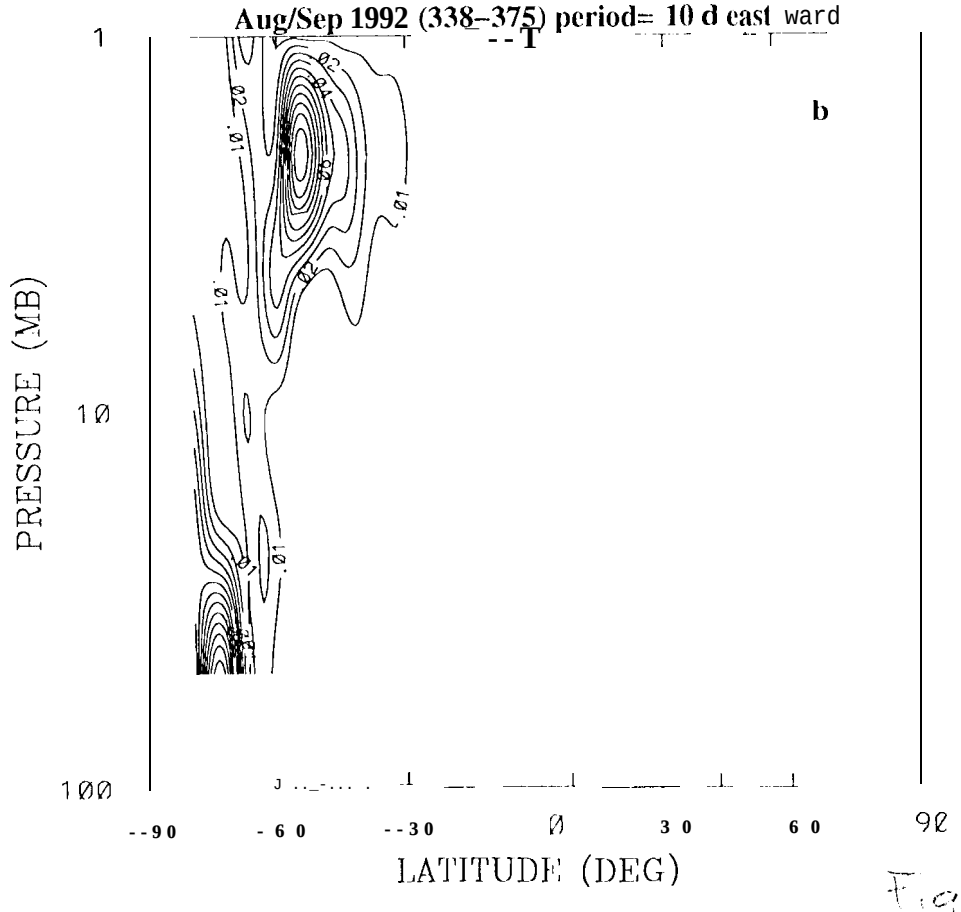
WAVE 1 MLS H_2O VARIANCE ($ppmv^2$)
Aug/Sep 1992 (338–375) period= 10 d eastward
b
1
10
100
PRESSURE (MB)
.02
.01
.05
.01
.02
.01
.01
.01
-90
-60
-30
0
30
60
90
LATITUDE (DEG)

Fig 7